

# Demonstration of negative differential resistance in GaN/AlN resonant tunneling diodes at room temperature

Z. Vashaei, C. Bayram, and M. Razeghi<sup>a)</sup>

*Department of Electrical Engineering and Computer Science, Center for Quantum Devices, Northwestern University, Evanston, Illinois 60208, USA*

(Received 4 January 2010; accepted 27 February 2010; published online 22 April 2010)

GaN/AlN resonant tunneling diodes (RTD) were grown by metal-organic chemical vapor deposition (MOCVD) and negative differential resistance with peak-to-valley ratios as high as 2.15 at room temperature was demonstrated. Effect of material quality on RTDs' performance was investigated by growing RTD structures on AlN, GaN, and lateral epitaxial overgrowth GaN templates. Our results reveal that negative differential resistance characteristics of RTDs are very sensitive to material quality (such as surface roughness) and MOCVD is a suitable technique for III-nitride-based quantum devices. © 2010 American Institute of Physics. [doi:10.1063/1.3372763]

## I. INTRODUCTION

During the last decades, III-nitride semiconductors have attracted immense attention owing to their outstanding properties such as wide bandgap energy, large bandgap discontinuity, high peak electron velocity, high saturation electron velocity, and high thermal stability. As a result, there has been great progress on the growth of optoelectronic devices based on III-nitride materials. The next step is realization of quantum devices using GaN-based material. Among the quantum devices, resonant tunneling diode (RTD) has attracted special interest.<sup>1,2</sup> RTDs are unique quantum devices allowing negative differential resistance (NDR) to be recognized at room temperature.<sup>3</sup> Thus, they are promising for high frequency generation up to terahertz enabling many applications such as ultraspeed wireless communications, spectroscopy, and imaging. GaN/AlN system with a large conduction band offset ( $\sim 2.1$  eV),<sup>4</sup> can provide high peak-to-valley ratio at room temperature, thus it is a suitable candidate for RTDs production.

Molecular beam epitaxy has been used for the growth of III-nitride RTDs,<sup>1,2</sup> however, there are no reports on room temperature NDR characteristics of RTDs grown by metal-organic chemical vapor deposition (MOCVD). Thickness controllability and smooth interface are crucially required for thin barrier RTD structures. To date, MOCVD has advantages in commercial production of nitride-based optoelectronic devices such as light emitting diodes, laser diodes, and detectors. However, achieving smooth heterojunctions as well as abrupt transition between nanoscale layers with a precise thickness control are still challenging issues for growth of GaN-based quantum effect devices<sup>1</sup> that might explain lack of RTDs grown by MOCVD.

In this work, MOCVD growth of GaN/AlN heterostructures has been systematically studied. Surface morphology and crystalline quality of GaN/AlN heterostructures have been investigated as a function of growth temperature, ammonia (NH<sub>3</sub>) flow rate, and indium (In) surfactant effect. The optimized growth conditions were employed for GaN/AlN

double barrier (DB) RTDs grown on different templates. Thanks to the material optimization, room temperature NDR characteristics of these RTDs were realized, and their dependence on templates were studied.

## II. EXPERIMENT

The growths were carried out in an AIXTRON 200/4-HT horizontal flow low-pressure MOCVD reactor. Trimethylaluminum (TMAI), trimethylgallium (TMGa), and trimethylindium (TMIn) were used as the metalorganic precursors for Al, Ga, and In, respectively. Silane was used as the *n*-type dopant source. Ammonia and a mixture of nitrogen and hydrogen were used as the anion source and carrier gases, respectively. All material optimizations have been performed at a pressure of 50 mbar on substrates composed of a 2- $\mu$ m-thick MOCVD-grown GaN on a double-side polished *c*-sapphire.

Realizing high quality GaN/AlN heterostructures are challenging due to different optimum growth conditions for AlN and GaN. Since AlN has relatively higher bonding energy than GaN, higher growth temperature [as high as 1200 °C (Ref. 5)] is favorable for high quality AlN epilayers in comparison to GaN [with favorable growth temperature of about 1050 °C (Ref. 6)]. Moreover, parasitic reactions occurring between TMAI and NH<sub>3</sub> necessitate lower pressure and V/III ratio for high quality AlN growth whereas higher pressure and V/III ratio are required for high quality GaN growth. Therefore, to grow high quality GaN/AlN heterostructures, deposition conditions simultaneously satisfying high quality growth conditions for both layers are required.

We investigated the effect of growth temperature, NH<sub>3</sub> flow rate, and surfactant effect (of indium) on surface morphology of single period GaN (2 nm)/AlN (1.5 nm) and crystalline quality of 50 period GaN (2 nm)/AlN (1.5 nm) superlattices (SLs). Atomic force microscopy (AFM) has been employed for surface morphology studies. High resolution x-ray diffraction (HRXRD) has been applied for crystalline quality investigation and constituent (AlN and GaN) layer thickness determination.

<sup>a)</sup>Electronic mail: razeghi@eecs.northwestern.edu.

TABLE I. Growth conditions and characterization results for single period GaN (2 nm)/AlN (1.5 nm) (A1–K1) and 50 period GaN (2 nm)/AlN (1.5 nm) SLs (A50–K50).

Sample identifier	Growth temperature (°C)	NH <sub>3</sub> flow rate (sccm)	In incorporation (%)	AFM rms roughness (nm)			(0002)XRD FWHM(arcsec)	
				1 × 1 μm <sup>2</sup>	5 × 5 μm <sup>2</sup>	10 × 10 μm <sup>2</sup>	GaN peak	0th peak
A1	910	1200	0	0.19	0.39	0.51		
A50							430	840
B1	950	1200	0	0.27	0.36	0.49		
B50							470	790
C1	990	1200	0	0.28	0.35	0.62		
C50							495	670
D1	1025	1200	0	0.34	0.41	0.48		
D50							445	580
E1	1070	1200	0	0.32	0.48	0.59		
F1	1100	1200	0	1.26	1.86	1.99		
G1	1025	1900	0	0.39	0.46	0.53		
H1	1025	900	0	0.35	0.51	0.69		
I1	1025	1200	~2% at GaN	0.38	0.58	0.65		
J1	1025	1200	~2% at AlN	0.25	0.47	0.74		
K1	1025	1200	~2% at	0.26	0.33	0.44		
K50			AlN/GaN				457	540

The optimum conditions for the growth of GaN/AlN heterostructures have been applied for growing DB RTD structures. The structure of DB RTDs will be explained in Sec. III B. Effect of templates on NDR characteristic of RTDs in view of surface roughness and dislocation density has been explored by growing RTDs on three different templates of GaN(2 μm), AlN (550 nm), and lateral epitaxial overgrowth (LEO) GaN(5 μm) (all grown on double-side polished c-sapphire). The LEO GaN template supplied to this work was previously grown as it is explained in Ref. 7. Device fabrication was realized via standard semiconductor processing techniques.<sup>8</sup>

### III. RESULTS AND DISCUSSION

#### A. GaN/AlN heterostructures growth optimization

Table I summarizes the root-mean-square (rms) roughness of (1 × 1), (5 × 5), and (10 × 10) μm<sup>2</sup> AFM scans of single GaN/AlN heterostructures as well as full-width-at-half-maximum (FWHM) of (0002) ω-2θ XRD of 50 period GaN/AlN SLs under various growth conditions. Letters (A–K) in Table I stand for GaN (2 nm)/AlN (1.5 nm) heterostructures grown under different conditions and indices (1 and 50) refer to the number of the heterostructure period.

Figure 1(a) shows AFM rms roughness of (1 × 1), (5 × 5), and (10 × 10) μm<sup>2</sup> scans of single GaN/AlN heterostructures as a function of growth temperature (910–1100 °C). Figures 1(b)–1(d) present typical AFM surface morphology for sample A1, D1, and F1 (see Table I) grown at 910 °C, 1025 °C, and 1100 °C, respectively. At 1100 °C, hillock formation dominates the surface. By decreasing growth temperature down to 1025 °C, smooth sawtooth like atomic steps appear on the surface and (5 × 5 μm<sup>2</sup>) rms roughness decreases from 1.86 to 0.41 nm (Table I). By further decrease in growth temperature down to

910 °C, atomic steps gradually vanish [Fig. 1(d)] and surface becomes nonuniform, possibly due to decrease in Al adatom mobility [compare rms roughness of (1 × 1), (5 × 5), and (10 × 10) μm<sup>2</sup> scans in Table I and Fig. 1(a)]. As Fig. 1(a) summarizes, the highest surface uniformity is achieved at 1025 °C, where rms roughness of largest area scan (10 × 10 μm<sup>2</sup>) is as small as 0.48 nm.

HRXRD is a nondestructive and relatively quick technique to investigate the structural properties of epitaxially grown heterostructures. However, structural investigation of very thin single-period heterostructures (about a few monolayers) using HRXRD is not feasible due to low diffraction intensity. One way to overcome this problem is investigating crystalline and interface quality of multiple-period heterostructures accumulating the x-ray diffraction (XRD) from

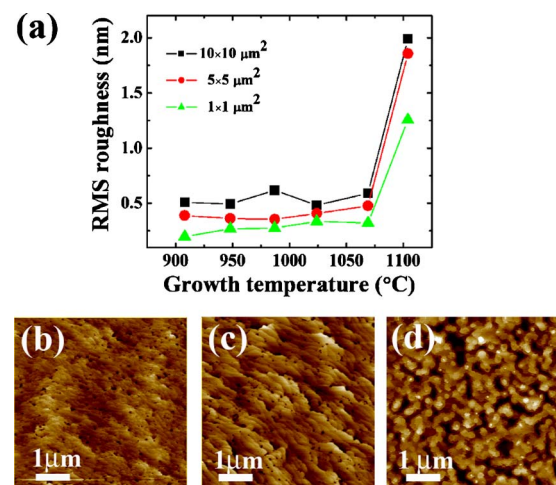


FIG. 1. (Color online) (a) rms roughness of GaN/AlN heterostructures as a function of growth temperature for different scan area. Typical AFM images of GaN/AlN heterostructure grown at (b) 910 °C (sample A1), (c) 1025 °C (sample D1), and (d) 1100 °C (sample F1).

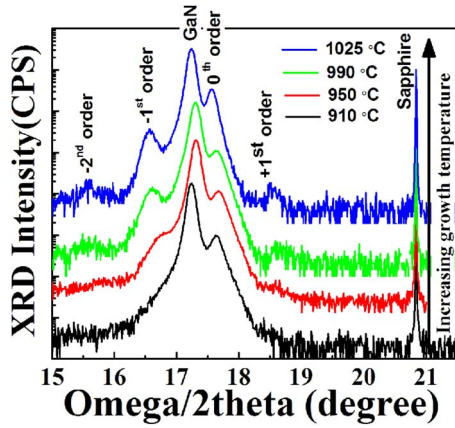


FIG. 2. (Color online) (0002)  $\omega$ - $2\theta$  XRD scans of 50 period of AlN/GaN SL structures grown at different temperatures (samples A50–D50).

multiple-interfaces.<sup>9</sup> Therefore, crystalline and interface quality of GaN/AlN heterostructures have been investigated by growing 50 period GaN /AlN SLs at various growth temperatures; same as single period GaN/AlN heterostructures (Table I, sample A50–D50). The satellite (interference) peaks are often observed at the  $\omega$ - $2\theta$  scans, with the spacing ( $\sin \theta_i - \sin \theta_j \cong \Delta\theta$ ) between two fringes  $i$  and  $j$  of order  $n$  being inversely related to the film thickness (for symmetric scans). Clearer fringes are obtained where there is more contrast between  $d$ -spacing of the two materials in the multilayers.<sup>10</sup> Figure 2 presents the  $\omega$ - $2\theta$  XRD scans of the SLs grown under different temperatures. For the GaN /AlN SLs grown at 950 °C or lower, no satellite peaks were observed. By increasing growth temperature, satellite peaks up to second order were observed indicating that SLs are in better crystalline quality and heterointerface between GaN and AlN layers are sharper. Density of screw dislocations ( $D_B$ ) in III-nitrides can be estimated from<sup>10</sup>

$$D_B = \beta^2/9b^2, \quad (1)$$

where  $\beta$  is FWHM of (0002) peak and  $b$  is the length of the burger vector of screw dislocations. Assuming Eq. (1), density of dislocations is proportional with the square of the FWHM, decreasing FWHM value clearly demonstrates a lower dislocation density in the material. As Table I shows, sample D1 grown at 1025 °C presents narrow XRD FWHMs for (0002) GaN peak (445 arcsec) as well as for the zero-order peak associated to SL (580 arcsec). This shows lower screw dislocation density and higher material quality. This growth temperature (1025 °C) is high enough to facilitate high mobility for Al adatoms and low enough to prevent Ga adatoms desorption and hillock formation [Fig. 1(d)]. Therefore, 1025 °C was determined to be the optimum growth temperature of GaN/AlN heterostructures enabling both high surface and crystalline quality and was employed for subsequent studies.

Ammonia flow rate is another growth parameter to be optimized for growing high quality GaN/AlN heterostructures. Therefore, the influence of  $\text{NH}_3$  flow rate on surface morphology of GaN/AlN heterostructures has been studied. The GaN/AlN heterostructures were grown under three different  $\text{NH}_3$  flow rates of 900, 1200, and 1900 sccm (sccm

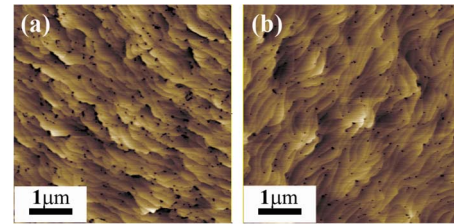


FIG. 3. (Color online) Effect of indium as a surfactant on the surface morphology of GaN/AlN heterostructure. AFM images of GaN/AlN heterostructure (a) without (sample D1) and (b) with indium (sample K1).

denotes standard cubic centimeter per minute at STP) (Table I, samples H1, D1, and G1) while TMGa and TMAI flow rates were fixed (at 12.5 sccm and 5.6 sccm, respectively). AFM ( $5 \times 5 \mu\text{m}^2$ ) rms roughness of samples H1, D1, and G1 are 0.51 nm, 0.41 nm, and 0.46 nm, respectively. The smoother and more uniform surface was achieved for the sample grown under 1200 SCCM. It is concluded that 1200 SCCM  $\text{NH}_3$  flow rate is the most favorable flow rate for the smooth GaN/AlN heterostructures.

Indium can enhance surface diffusion length of Al and Ga adatom by decreasing diffusion barrier of nitrogen adatoms.<sup>11</sup> We supplied TMI along with TMAI and/or TMGa to investigate the effect of indium on surface morphology and crystalline quality of GaN/AlN heterostructures.

Sample I1 (with indium incorporation at GaN layer) and J1 (with indium incorporation at AlN layer), has an rms roughness of 0.58 nm and 0.47 nm, respectively, however, sample K1, where indium introduced to both AlN and GaN layer of GaN/AlN heterostructure, has an rms roughness of 0.33 nm ( $5 \times 5 \mu\text{m}^2$ ) (Table I). Figure 3 displays AFM images of GaN/AlN heterostructure with (sample K1) and without (sample D1) indium incorporation. The  $5 \times 5 \mu\text{m}^2$  rms roughness decreases from 0.41 to 0.33 nm by introducing indium. No significant variation on FWHM of (0002) peaks of GaN and zero-order peaks of SL (sample D2 and K2) suggesting that indium improves the surface morphology with the least incorporation in crystalline structure. In summary, smoother GaN/AlN heterostructure surface was achieved when indium was introduced during the deposition of both AlN and GaN layers. Our results are in good agreement with previous reports where indium was employed to improve quality of GaN/AlN multiquantum wells.<sup>12</sup>

## B. Growth of GaN/AlN DB RTDs

Precise control over layer thicknesses is a challenge to be addressed for realization of RTDs. The growth rate of thick bulk layers is not directly applicable for nano-scale films as thinner layers are more prompt to degradation by means of decomposition, desorption, and diffusion.<sup>13</sup> Therefore thickness calibration has been done by growing 50 period AlN/GaN SLs (using optimized conditions explained in Sec. III A) via varying the deposition time of GaN (AlN) while keeping the AlN (GaN) deposition time constant.

For the superlattice structures, the angular separation between satellite peaks can be used to calculate the SL period ( $P_{SL}$ ) via<sup>10</sup>

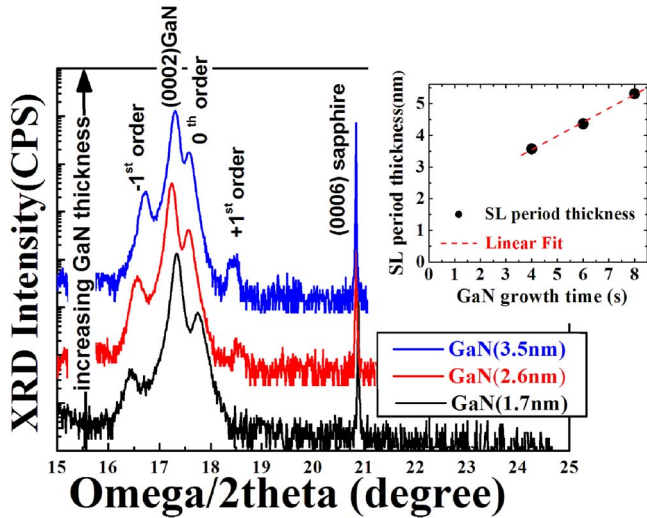


FIG. 4. (Color online) Thickness calibration of GaN/AlN heterostructure. (0002)  $\omega$ - $2\theta$  XRD scans of 50 period of AlN/GaN SL structures with different GaN thicknesses (1.7, 2.6, and 3.5 nm) and constant AlN thickness (1.9 nm). The inset shows the SL period as a function of GaN growth time.

$$P_{\text{SL}} = \frac{(n_i - n_j)\lambda}{2(\sin \theta_i - \sin \theta_j)} \approx \frac{\lambda}{2\Delta\theta \times \cos(\theta_{\text{SL}}^B)}, \quad (2)$$

where  $\lambda$ ,  $\Delta\theta$ , and  $\theta_{\text{SL}}^B$  are the wavelength of the incident x-ray, angular separation between two adjacent satellite peaks, and the Bragg angle of the SL (the position of the 0th order satellite peak). From the deduced  $P_{\text{SL}}$ , the constituent AlN and GaN layer thicknesses are calculated.  $\omega$ - $2\theta$  XRD scans of three calibration SLs composed of 1.7, 2.6, and 3.5-nm-thick GaN (all employing 1.9-nm-thick AlN) are given in Fig. 4. Thickness calibration has been repeated for SLs composed of 0.9, 1.9, and 2.9-nm-thick AlN (all employing 2.6-nm-thick GaN) (not shown here). The inset of Fig. 4 shows the SLs period as a function of GaN deposition time. The growth rates of AlN and GaN extracted from slope of linear fitting were determined as 0.33 Å/sec and 4.34 Å/sec, respectively.

RTDs performance is very sensitive to material quality. In order to demonstrate that our optimized GaN/AlN heterostructures are high quality, they are employed as active layers in DB RTDs. First, 500-nm-thick Si-doped GaN (with a carrier concentration of  $4 \times 10^{18} \text{ cm}^{-3}$ ) was regrown at 100 mbar on the templates to act as the  $n$ -contact region of RTD. Then, active layer composed of 2 nm GaN/1 nm AlN/0.8 nm GaN/1 nm AlN/2 nm GaN was regrown on  $n$ -GaN. The undoped 2 nm GaN was inserted before and after the DB GaN/AlN layer to act as spacer layers between highly doped bottom and top contact layers and undoped DB layer. This active layer was capped with 300 nm  $n$ -GaN to form the top  $n$ -contact region, under the same growth conditions of bottom  $n$ -contact. Figures 5(a) and 5(e) show sketch of RTD structure before and after capping with top  $n$ -contact. In order to investigate the effect of template on RTD performance, three different templates of GaN (2  $\mu\text{m}$ ), AlN (550 nm), and LEO GaN (5  $\mu\text{m}$ ) (all on double-side polished c-sapphire) have been applied to grow RTD structure on.

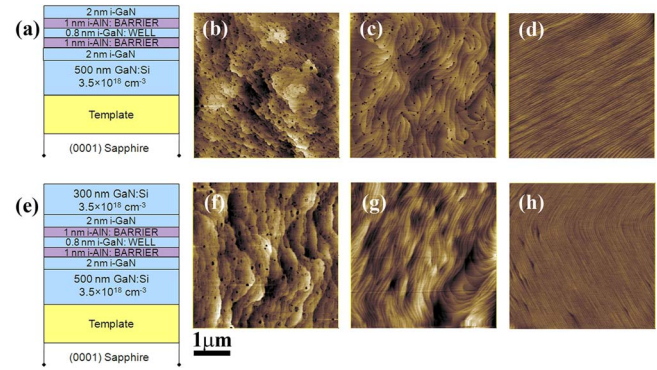


FIG. 5. (Color online) (a) Sketch of RTD structure up to active layer and its typical AFM image, (b) on AlN template (with rms of 0.77 nm), (c) on GaN template (with rms of 0.30 nm), (d) on the wing region of LEO GaN (with rms of 0.13 nm). (e) sketch of completed device and its typical AFM image, (f) on AlN template (with rms of 0.78 nm), (g) on GaN template (with rms of 0.41 nm), and (h) on the wing region of LEO GaN (with rms of 0.11 nm).

Typical ( $5 \times 5 \mu\text{m}^2$ ) AFM images of the active layer surface and the completed RTD surface grown on AlN (550 nm), GaN (2  $\mu\text{m}$ ), and on the wing region (where the lateral growth occurs) of LEO GaN template are given in Figs. 5(b)–5(d) and 5(f)–5(h), respectively. The atomic steps are observed for all layers; however, surface of RTD grown on the wing region of LEO GaN template is much smoother than those grown on two other templates. The rms roughness of active layer surface and completed RTD surface are 0.13 and 0.11 nm for RTD grown on the wing region of LEO GaN whereas those values for RTDs grown on GaN template are 0.30 and 0.41 nm and on AlN template are 0.77 nm and 0.78 nm respectively. Moreover, dark spots in AFM images corresponding to the intersection of screw dislocations with the surface decrease from layers grown on AlN template to GaN template and LEO GaN template, indicating lowest dislocation density in layers grown on LEO GaN template.

RTDs with mesa size of 15  $\mu\text{m}$  diameter were fabricated under standard semiconductor processing techniques<sup>5</sup> and their NDR characteristics were studied. Room temperature current-voltage (I-V) characteristics were obtained by probing the devices. I-V curves were measured using an HP4155A semiconductor parameter analyzer configured to input a voltage sweep while measuring current. Figure 6 shows room temperature I-V curves of three RTDs (grown

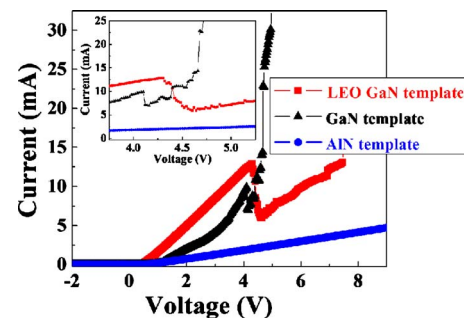


FIG. 6. (Color online) Room temperature I-V curves, taken by sweeping voltage in positive direction while measuring current, of RTDs grown on different templates of AlN, GaN, and LEO GaN. Inset is a magnified display of NDR region.

on different templates) taken by sweeping the voltage from  $-2$  up to  $7$  V while measuring the current through the devices. NDR can be observed for devices fabricated on LEO GaN and GaN template while RTD devices on AlN template did not show NDR characteristics. For devices fabricated on LEO GaN, NDR is observed at  $4.3$  V with a peak-to-valley ratio (P/V) of about  $2.15$  and for those RTDs fabricated on GaN template NDR is observed at  $4.1$  V with P/V of about  $1.42$  (see Fig. 6).

It is well known that  $V_{\text{NDR}}$  and P/V are significantly affected by heterointerface roughness within RTDs [as shown in AlGaAs/GaAs RTDs (Ref. 14)]. Considering the strong polarization in III-nitrides, effect of interface roughness is expected to be more important. The effect of surface roughness and dislocation density on RTD performance can clearly be observed for RTDs grown on different templates (see Fig. 5). For the RTD grown on LEO GaN, NDR possesses highest P/V due to lowest surface roughness and dislocation density. For the RTD grown on AlN template, NDR was not observed due to rough surfaces and high dislocation density. This suggests that RTDs are very sensitive to surface roughness and dislocations and NDR can be observed from high quality GaN/AlN heterostructures grown only on very high quality templates.

#### IV. CONCLUSION

We have demonstrated room temperature NDR in GaN/AlN RTDs by MOCVD. Optimized growth conditions have been applied for the growth of DB RTDs on AlN, GaN, and LEO GaN templates. Room temperature peak-to-valley ratio of about  $2.15$  and  $1.42$  has been achieved for RTDs grown on LEO GaN and GaN template, however, no NDR characteristics has been observed for RTDs grown on AlN template. It is shown that NDR is very sensitive to dislocations and sur-

face roughness. Our results demonstrate that high quality GaN/AlN heterointerfaces can be achieved by material optimization and MOCVD is a promising technique for growing quantum devices such as RTDs.

#### ACKNOWLEDGMENTS

The authors acknowledge valuable collaboration with Dr. S. R. Darvish and B. M. Nguyen regarding fabrication, all from Center for Quantum Devices at Northwestern University, and Dr. J. Zavada of ARO, Dr. J. Mangano and Dr. Scott Rodgers of DARPA, and Mr. Jerry Speer of U.S. Army RDECOM for their interest and encouragement.

- <sup>1</sup>A. Kikuchi, R. Bannai, K. Kishino, C.-M. Lee, and J.-I. Chyi, *Appl. Phys. Lett.* **81**, 1729 (2002).
- <sup>2</sup>S. Golka, C. Pflügl, W. Schrenk, G. Strasser, C. Skierbiszewski, M. Siekacz, I. Grzegory, and S. Porowski, *Appl. Phys. Lett.* **88**, 172106 (2006).
- <sup>3</sup>L. L. Chang, L. Esaki, and R. Tsu, *Appl. Phys. Lett.* **24**, 593 (1974).
- <sup>4</sup>G. Martin, S. Strite, A. Botchkarev, A. Agarwal, A. Rockett, H. Morkoc, W. R. L. Lambrecht, and B. Segall, *Appl. Phys. Lett.* **65**, 610 (1994).
- <sup>5</sup>Y. A. Xi, K. X. Chen, F. Mont, J. K. Kim, C. Wetzel, E. F. Schubert, W. Liu, X. Li, and J. A. Smart, *Appl. Phys. Lett.* **89**, 103106 (2006).
- <sup>6</sup>R. Chierchia, T. Böttcher, H. Heinke, S. Einfeldt, S. Figge, and D. Hommel, *J. Appl. Phys.* **93**, 8918 (2003).
- <sup>7</sup>C. Bayram, J. L. Pau, R. McClintock, and M. Razeghi, *Appl. Phys. B: Lasers Opt.* **95**, 307 (2009).
- <sup>8</sup>C. Bayram, Z. Vashaei, M. Razeghi, *Appl. Phys. Lett.* **96**, 042103 (2010).
- <sup>9</sup>M. E. Vickers, M. J. Kappers, T. M. Smeeton, E. J. Thrush, J. S. Barnard, and C. J. Humphreys, *J. Appl. Phys.* **94**, 1565 (2003).
- <sup>10</sup>M. A. Moram and M. E. Vickers, *Rep. Prog. Phys.* **72**, 036502 (2009).
- <sup>11</sup>J. Neugebauer, *Phys. Status Solidi C* **0**, 1651 (2003).
- <sup>12</sup>S. Nicolay, E. Feltin, J.-F. Carlin, M. Mosca, L. Nevou, M. Tcherynecheva, F. H. Julien, M. Ilegems, and N. Grandjean, *Appl. Phys. Lett.* **88**, 151902 (2006).
- <sup>13</sup>N. Gogneau, D. Jalabert, E. Monroy, E. Sarigiannidou, J. L. Rouvie' re, T. Shibata, M. Tanaka, J. M. Gerard, and B. Daudin, *J. Appl. Phys.* **96**, 1104 (2004).
- <sup>14</sup>H. C. Liu and D. D. Coon, *J. Appl. Phys.* **64**, 6785 (1988).